Shallow and deep donors in direct-gap n-type $Al_xGa_{1-x}As$:Si grown by molecular-beam epitaxy

E. F. Schubert and K. Ploog
Max-Planck-Institut für Festkörperforschung, D-7000 Stuttgart 80, Federal Republic of Germany
(Received 21 May 1984)

Temperature-dependent Hall-effect measurements are reported and analyzed in detail for n-type $Al_xGa_{1-x}As$ of composition $0 \leq x \leq 0.40$ grown by molecular-beam epitaxy and highly doped with Si ($N_{Si} \geq 5\times10^{17}$ cm^{-3}). A quantitative analysis using Fermi-Dirac statistics reveals for the composition range $0.20 \leq x \leq 0.40$ the presence of a hydrogenlike shallow Si donor which interacts with the Γ valley and a deep Si donor related to the X valley. In contrast to previous results, the thermal activation energy of the deep donor, determined to be $E_{dd} = 140 \pm 10$ meV, does not change significantly with alloy composition. Only the ratio of shallow- to deep-donor concentration depends on composition. For $x \leq 0.20$, neither deep-donor nor persistent photoconductivity exists in n-type $Al_xGa_{1-x}As$:Si. For $0.20 \leq x \leq 0.40$, however, the deep-donor concentration increases with x while simultaneously the shallow-donor concentration decreases. The proposed interaction of the deep donor with the X valley helps in understanding the persistent photoconductivity found in n-type $Al_xGa_{1-x}As$ with $0.20 \leq x \leq 0.40$.

I. INTRODUCTION

In this paper we analyze in detail the temperature dependence of Hall-effect measurements performed on Si-doped direct-gap n-type $Al_xGa_{1-x}As$ layers ($0 \leq x \leq 0.40$, $N_{Si} \geq 5\times10^{17}$ cm^{-3}) grown by molecular-beam epitaxy (MBE). The dominant features of this temperature dependence are as follows. (a) At low Al content (i.e., $x \leq 0.2$), the transport properties of n-type $Al_xGa_{1-x}As$:Si are similar to those of n-type GaAs:Si except for the reduced mobility caused by alloy scattering.[1,2] The observed net-electron concentration closely follows the overall Si concentration incorporated, and no carrier freeze-out occurs upon cooling to 4.2 K. (b) With increased Al content ($0.20 \leq x \leq 0.40$), a significant reduction of the 300-K free-electron concentration as compared to the Si concentration incorporated is observed.[2,3] In the dark, a substantial carrier freeze-out is found upon cooling, until at $T \leq 100$ K the carrier concentration remains constant.[2,4,5] (c) In addition, persistent photoconductivity (PPC) arises in this composition range below 100 K.[6] The intensity of PPC depends strongly on the doping level and on the layer thickness.[2]

These distinct phenomena are not unique to MBE-grown n-type $Al_xGa_{1-x}As$:Si layers. Similar results have been obtained for n-type $Al_xGa_{1-x}As$ grown by liquid-phase epitaxy (LPE) or metal organic chemical vapor deposition (MOCVD) and doped with Se,[7] Te,[8] or Sn,[9] respectively. It is therefore generally accepted that the features observed in the composition range $0.20 \leq x \leq 0.40$ are fundamental material properties of the ternary alloy $Al_xGa_{1-x}As$ which are most probably caused by a homogeneously distributed deep center involving the specific donor atom used for doping. Lang *et al.*[10] designated this center as "*DX*" and proposed that the *DX* center is a complex involving a donor atom and an anion vacancy.

The model of *DX* centers in n-type $Al_xGa_{1-x}As$ has raised two important questions. *First,* the center must undergo a large lattice relaxation with the capture or emission of an electron at the defect. The authors had to assume a non-effective-mass framework to explain the existence of this particular defect state, which is resonant with the conduction band when not occupied, but which relaxes deep into the gap after the capture of an electron. *Second,* the model requires anion, i.e., As, vacancies to establish the microstructure of the *DX* center, irrespective on the growth mode used for the n-doped $Al_xGa_{1-x}As$ and the lattice site occupancy of the specific donor impurity (Sn, Si on Ga sites, and Se, Te on As sites, respectively). The presence of As vacancies is plausible for materials grown from a Ga solution during LPE. However, the existence of As vacancies become unlikely in n-type $Al_xGa_{1-x}As$ grown by MBE or MOCVD which both operate with a rather high excess arsenic flux.

Considering the microstructure of the *DX* center we have therefore in detail evaluated new experimental data obtained from temperature-dependent Hall-effect measurements on direct-gap n-type $Al_xGa_{1-x}As$:Si. For the range $0.20 \leq x \leq 0.40$ a quantitative analysis using Fermi-Dirac statistics reveals the existence of a hydrogenlike *shallow* donor interacting with the Γ valley and of a simple *deep* donor related to the X valley, which are both associated directly with the Si doping impurity. While the ratio of the deep- to shallow-donor concentration increases with the Al content x, the thermal activation energy of $E_{dd} = 140 \pm 10$ meV for the deep donor remains nearly constant. The accurate determination of this activation energy requires a substantial modification of the simple relation $n \sim \exp(-E_{dd}/kT)$ by including the shallow-donor concentration in the analysis. Our analysis proposes further that the PPC effect in the n-type $Al_xGa_{1-x}As$ with $0.20 \leq x \leq 0.40$ follows directly from the relation of the deep donor to the X valley, i.e., from the specific band structure of the ternary alloy. A donor complex involving donor atom plus an anion vacancy is not required for the interpretation of the temperature-

dependent Hall-effect data.

In Sec. II we will present the experimental methods and in Sec. III A we will describe and discuss the experimental results on temperature-dependent Hall-effect measurements which will be analyzed in Secs. III B and III C. In Sec. III D we will discuss the influence of alloy composition, and in Sec. IV we will summarize the results.

II. EXPERIMENTAL

The Si-doped direct-gap n-type $Al_xGa_{1-x}As$ layers used in this study were grown in an MBE system of the quasihorizontal evaporation type which includes a continuously azimuthally rotating substrate holder and a liquid N_2 cryoshroud encircling the growth region. The ternary alloy material with a thickness of 2–3 μm was deposited on [100]-oriented semi-insulating GaAs substrates at a growth temperature from 630 to 670 °C in different growth runs. Details of the growth procedure for intentional variation of the alloy composition and doping concentration have been described elsewhere.[2,5] Care was taken to avoid the formation of electron conducting channels in the GaAs substrate adjacent to the $Al_xGa_{1-x}As$/GaAs interface which could falsify the measured transport properties.[2] For comparison, additional samples were grown having either a barrier of higher Al-mole fraction at the substrate-epitaxial layer interface or an intentional two-dimensional electron gas (2D EG) at the interface to prove conclusively the absence of a 2D EG in the samples described here. Doping concentrations in excess of 1×10^{17} cm^{-3} were chosen, because this range is important for application of the ternary alloy in selectively doped n-type $Al_xGa_{1-x}As$/GaAs heterostructures used for the fabrication of high electron mobility transistors where the PPC effect is highly undesirable. The incorporated Si concentration N_{Si} was determined from Si-doped GaAs layers grown at similar growth rates in which N_{Si} corresponds directly to the observed electron concentration. The material quality and the Al content of the samples were examined by low-temperature photoluminescence measurements[11] and complementary by Raman scattering experiments.[12]

For the Hall-effect measurements the samples were defined photolithographically and etched into Hall bars with current contacts at both ends and six potential probes. The ohmic contacts were formed by carefully alloying small balls of Sn into the samples. The Hall effect was measured at a magnetic induction of 0.5 T in the temperature range 4.2 to 300 K using a fully automated system. The sample was mounted on a Cu block in a variable temperature continuous He flow cryostat. The flow rate of liquid He, the setting of the temperature controller, and the reversion of the polarity of the magnetic field were all set and controlled by a programmable desk-top calculator. For illumination of the sample we used a GaAs light-emitting diode (LED) with a wavelength of $\lambda=820$ nm. The energy of the photons emitted from this incoherent monochromatic light source is smaller than the band gap of $Al_xGa_{1-x}As$ so that excitation of electrons from the valence to the conduction band in the ternary material can be excluded.

The actual free-electron concentration n and the inverse Hall coefficient divided by the elementary charge, $1/qR_H$ (i.e., the Hall carrier concentration), are not equal. The difference of the two values is given by the Hall factor r_H, which depends on the predominant scattering mechanism, on the conduction-band structure, and on the mobility of the Γ, L, and X valleys, because the electrons may be distributed among the various minima. Corrections were not made to the $1/qR_H$ values for our analysis, owing to uncertainties in the band structure and in the respective mobilities, and we thus refer to the Hall electron concentration throughout the text.

III. RESULTS AND DISCUSSION

A. Temperature dependence of Hall-effect measurements

Nominally undoped $Al_xGa_{1-x}As$ layers grown in the MBE system used for the present study are p type with net carrier concentration below 10^{15} cm^{-3} at 300 K due to residual carbon acceptors. Doping of MBE-grown $Al_xGa_{1-x}As$ with Si yields n-type conductivity over the entire alloy composition range studied here. For $0\le x\le0.20$ the measured Hall electron concentration in n-type $Al_xGa_{1-x}As$:Si is proportional to the overall Si concentration incorporated.[1,2] In the entire temperature range $4.2\le T\le300$ K we observe *no* carrier freeze-out for doping concentrations $N_{Si}\ge10^{16}$ cm^{-3}. In analogy to n-type GaAs:Si we can thus attribute the free-electron concentration found in n-type $Al_xGa_{1-x}As$:Si with $0\le x\le0.20$ to ionized shallow Si-donors associated with the Γ minimum of the conduction band. According to the hydrogen-atom model used for n-type GaAs, the shallow donor has a ground-state energy of $E_{sd}=5.3$ meV below the conduction band. Spectra of far-infrared extrinsic photoconductivity yielded a value of $E_{sd}=5.86$ meV.[13] The good agreement of both values implies that the hydrogen-atom model applies very well to the shallow Si donor impurity in GaAs. This donor does not freeze-out, because at doping concentrations $N_{Si}\ge10^{16}$ cm^{-3} the energy separation between ground state and excited states of the shallow hydrogen-atom-like donors, which form a quasicontinuum, is negligibly small[13] (overlap of Coulomb potentials, i.e., Mott transition). Hall-effect measurements on n-type $Al_xGa_{1-x}As$:Si with $0\le x\le0.20$ determine the thermal activation energy of the shallow donor at these fairly high doping levels to be zero.

The temperature-dependent Hall data change drastically when we increase the Al content in n-type $Al_xGa_{1-x}As$:Si to $x\ge0.20$. Figures 1 and 2 show the results of measurements made on two representative 2.5-μm-thick Si-doped n-type $Al_xGa_{1-x}As$ films of composition $x=0.25$ ($N_{Si}\simeq9\times10^{17}$ cm^{-3}) and $x=0.32$ ($N_{Si}\simeq1.5\times10^{18}$ cm^{-3}). The data designated "dark" were measured without any exposure to light, whereas the data designated "illum." were measured in the dark after exposing the sample to monochromatic incoherent light of wavelength $\lambda=820$ nm at 4.2 K until the carrier concentration has reached its saturated value in order to produce persistent photoconductivity. In the dark, the Hall electron concentration decreases exponentially as the tempera-

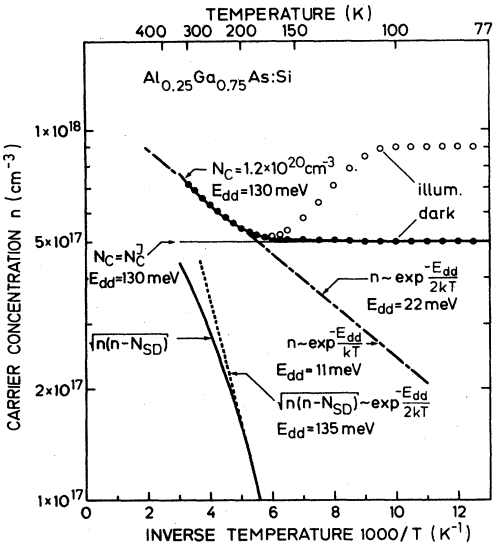

FIG. 1. Dependence of the Hall electron concentration in n-type $Al_{0.25}Ga_{0.75}As$:Si on inverse lattice temperature. Solid and open circles indicate experimental data measured in the dark and after illumination at low temperatures, respectively. The deep-donor thermal activation energy E_{dd} is evaluated by three methods. The simple relations $n \sim \exp(-E_{dd}/kT)$ and $n \sim \exp(-E_{dd}/2kT)$ yield $E_{dd}=11$ and 22 meV, respectively (dashed-dotted line). A more realistic value of $E_{dd}=135$ meV is obtained using the relation $(n^2-nN_{SD})^{1/2} \sim \exp(-E_{dd}/2kT)$ at low temperature indicated by the dotted line. A simulation of the carrier concentration versus temperature in terms of Fermi-Dirac statistics yielding $E_{dd}=130$ meV for the thermal activation energy of the deep donor (solid curve) coincides with the experimental data only if a density of states much larger than that of the Γ valley is used. As indicated, the experimental data cannot be fitted to the experimental data by means of the lower joint density of states N_C^J.

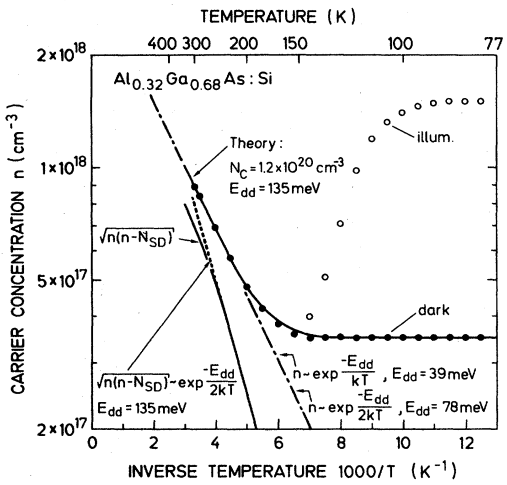

FIG. 2. Dependence of the Hall electron concentration in n-type $Al_{0.32}Ga_{0.68}As$:Si on inverse lattice temperature. Solid and open circles indicate experimental data measured in the dark and after illumination at low temperatures, respectively. The deep-donor thermal activation energy E_{dd} is evaluated by three methods. The simple relations $n \sim \exp(-E_{dd}/kT)$ and $n \sim \exp(-E_{dd}/2kT)$ yield $E_{dd}=39$ and 78 meV, respectively (dashed-dotted line). A more realistic value of $E_{dd}=135$ meV is obtained using the relation $(n^2-nN_{SD})^{1/2} \sim \exp(-E_{dd}/2kT)$ at low temperature indicated by the dotted line. A simulation of the carrier concentration versus temperature in terms of Fermi-Dirac statistics yielding $E_{dd}=135$ meV for the thermal activation energy of the deep donor (solid curve) coincides with the experimental data only if a density of states much larger than that of the Γ valley is used.

ture decreases, due to a partial carrier freeze-out into a deep level.[2,4–6] At temperatures below 150 K, the Hall electron concentration saturates at a level of 5×10^{17} cm^{-3} in Fig. 1 and 3.5×10^{17} cm^{-3} in Fig. 2 (below 77 K the Hall carrier concentration in the dark and after illumination remains constant; therefore, the temperature range down to 4.2 K is not shown in the figures). This saturated Hall electron concentration detected in the dark at low temperatures originates from shallow Si donors related to the Γ minimum comparable to the Si donor in the composition range $0 \leq x \leq 0.20$.

A deep donor exists in addition, however, for alloy compositions $0.20 \leq x \leq 0.40$ whose nature will be interpreted in the following sections. The carrier-concentration—versus—inverse-temperature dependence in the dark shown in Figs. 1 and 2 is a general feature of the n-doped ternary alloy $Al_xGa_{1-x}As$ with $0.20 \leq x \leq 0.40$ which does *not* depend on the growth mode and on the donor impurity used. Only the slope of $\ln(n)$ versus $1/T$ and the saturated electron concentration in the dark are modified by variation of the alloy composition and of the overall doping concentration (see also Figs. 1 and 2).[5]

After exposure of the sample to light of energy below the band gap of $Al_xGa_{1-x}As$, the Hall electron concentrations in Figs. 1 and 2 strongly increase at low temperature to saturated values, which at 77 K are even higher than the 300-K value measured before illumination. Further illumination no longer increases the carrier concentrations. The measured increase of the carrier concentrations persists even for days after returning the samples to the dark at low temperatures. This phenomenon is called "persistent photoconductivity" (PPC) in n-type $Al_xGa_{1-x}As$ with $x \geq 0.20$. At a given alloy composition x the amount of photoexcited carriers is directly proportional to the doping concentration and to the thickness of the epitaxial layer. We therefore assume that PPC directly correlates with the donor impurities in n-type $Al_xGa_{1-x}As$, which provide some microscopic barrier to prevent recapture of photoexcited free electrons. These features have already been discussed in Refs. 2, 5, and 10. We will subsequently show in detail that the donor responsible for PPC is much deeper than the donor responsible for the saturated dark electron concentration. This deep donor is ionized optically at low temperatures yielding PPC and thermally at higher temperatures (see also Figs. 1 and 2 for illustration).

In n-type $Al_xGa_{1-x}As$:Si of composition $0.20 \leq x \leq 0.40$, we must thus discriminate between two types of donors, a shallow one and a deep one, whose concentration ratio depends primarily on the alloy composition (see Sec. III D). The concentration of the deep donor, N_{DD},

can be deduced from the PPC concentration (after light exposure and at low temperature), n_{PPC}, and the low-temperature concentration in the dark which corresponds to the shallow-donor concentration N_{SD}, i.e.,

$$N_{DD}=n_{PPC}-N_{SD} . \quad (1)$$

The quantity $(N_{SD}+N_{DD})$ coincides with the incorporated Si concentration N_{Si}. Inspection of Figs. 1 and 2 reveals a considerable difference between the PPC concentration n_{PPC} and the 300-K concentration. This discrepancy demonstrates that even at room temperature the deep donor is not completely ionized.

B. Thermal activation energy of the deep donor

In a number of papers published previously[1,3,4,6,7] the thermal activation energy of the donor level E_{dd} was evaluated from Hall data according to the relation

$$n\sim\exp(-E_{dd}/kT) \quad (2a)$$

for its low-temperature approximation, and

$$n\sim\exp(-E_{dd}/2kT) \quad (2b)$$

for its high-temperature approximation (de Boer—van Geel relation). In this way the authors had obtained a large range of donor activation energies (from 0 to 150 meV) which seemed to depend strongly on the alloy composition. For our sample of Fig. 1 the thermal activation energy would be $E_{dd}=11$ meV and $E_{dd}=22$ meV, using Eqs. (2a) and (2b), respectively, and for the sample in Fig. 2, $E_{dd}=39$ meV and $E_{dd}=78$ meV, respectively. We will now show that the E_{dd} values obtained from Eqs. (2a) and (2b) represent only apparent donor activation energies arising from an averaging of the actual deep- and shallow-donor levels and their respective concentrations at a given alloy composition x.

Fermi-Dirac statistic gives the concentration of ionized deep donors, N_{DD}^{+}, according to

$$N_{DD}^{+}=N_{DD}\left\{1-\left[1+\frac{1}{g}\exp\left[-\frac{E_F-E_{DD}}{kT}\right]\right]^{-1}\right\}, \quad (3)$$

where N_{DD} is the overall deep-donor concentration, g is the ground-state degeneracy of the donor, and E_F and E_{DD} are the Fermi and the actual deep-donor energy, respectively. Maxwell-Boltzmann statistics for the conduction band yields

$$n=N_C\exp[-(E_C-E_F)/kT] , \quad (4)$$

where N_C is the effective density of states at the conduction-band edge, and E_C is the conduction-band energy. For the occupation of the conduction band we use Maxwell-Boltzmann statistics to get a formula in closed form. Elimination of E_F yields the quadratic equation

$$(N_{DD}^{+})^2+N_{DD}^{+}(N_C'+N_{SD})-N_{DD}N_C'=0 , \quad (5)$$

where

$$N_C'=\tfrac{1}{2}N_C\exp[-(E_C-E_{DD})/kT] . \quad (6)$$

With $E_{dd}=E_C-E_{DD}$ (the deep-donor ionization energy E_{dd} is taken relative to the conduction-band edge) and the inequality $N_C'\ll N_{SD}$, the following simple relation is obtained:

$$n^2-nN_{SD}\sim\exp(-E_{dd}/kT) , \quad (7)$$

where the free-electron concentration n is the sum of shallow-donor plus *ionized* deep-donor concentration. Equation (7) clearly shows that the shallow-donor concentration N_{SD} has to be included in the accurate evaluation of the thermal activation energy of the deep donor.

It is possible to obtain Eq. (7) also via the law of mass action. If we consider the ionization of the donors as a chemical reaction according to

$$N_{SD}+N_{DD}\leftrightarrow N_{SD}^{+}+N_{DD}^{+}+n , \quad (8)$$

the law of mass action is easily applied:

$$(N_{SD}^{+}N_{DD}^{+}n)/(N_{SD}N_{DD})=CT^3\exp(-E_{dd}/kT) . \quad (9)$$

Since the shallow donor is ionized at all temperatures, we obtain the relation

$$(n^2-nN_{SD})^{1/2}\sim\exp(-E_{dd}/2kT) . \quad (10)$$

This equation is identical to Eq. (7), so that we obtain the same result using two independent methods.

We now determine the activation energy of the deep donor for the sample displayed in Figs. 1 and 2, using Eqs. (7) and (10), and compare the result with the values obtained via Eqs. (2a) and (2b). For this purpose we plot the square root of n^2-nN_{SD} versus inverse temperature in the figures. The slope of $(n^2-nN_{SD})^{1/2}$ vs $1/T$ has to be evaluated for a temperature range where the deep donor is ionized only weakly, because Eq. (7) was derived for $N_C'\ll N_{SD}$, i.e., at low temperatures. As indicated in Figs. 1 and 2 we deduce an activation energy of $E_{dd}=135$ meV for the deep donor by this procedure for both alloy compositions. This value is much larger than the energies obtained from Eqs. (2a) and (2b), respectively. If the shallow-donor concentration N_{SD} is not included in the evaluation, the actual value of E_{dd} is obviously greatly underestimated, particularly at lower x values, and it apparently depends on the alloy composition x. In the next section we will demonstrate that the use of Eq. (7) or (10), respectively, yields quite realistic values for the deep-donor activation energy in n-type $Al_xGa_{1-x}As$:Si with $0.20\le x\le 0.40$.

C. Analysis of temperature-dependent Hall-effect data

For a more detailed analysis of the temperature dependence of the Hall-effect measurements on n-type $Al_xGa_{1-x}As$:Si with $0.20\le x\le 0.40$ we use Fermi-Dirac statistics for the deep donor as well as for the occupation of the conduction band. Several analytic approximations have been developed for the Fermi-Dirac integral, in order to avoid numerical solutions. Valid to the highest degree of degeneracy is the Joyce-Dixon approximation:[14]

$$(E_F-E_C)/kT=\ln\frac{n}{N_C}+\sum_{m=1}^{4}A_m\left[\frac{n}{N_c}\right]^m . \quad (11)$$

The coefficients A_m are given by

$$A_1 = 3.535\,53 \times 10^{-1},$$
$$A_2 = -4.950\,09 \times 10^{-3},$$
$$A_3 = 1.483\,86 \times 10^{-4}, \tag{12}$$
$$A_4 = -4.425\,63 \times 10^{-6}.$$

Together with Fermi-Dirac statistics for the deep donor [Eq. (3)] we obtain

$$N_{DD}^{+} = N_{DD}\left\{1 + g\exp\left[\sum_{m=1}^{4} A_m \left[\frac{n}{N_C}\right]^m\right]\frac{n}{N_C}\exp\frac{E_{dd}}{kT}\right\}^{-1}. \tag{13}$$

The free-carrier concentration n is obtained via the sum of the shallow-donor concentration N_{SD} and the ionized deep-donor concentration N_{DD}^{+}, given by Eq. (13) according to

$$n = N_{SD} + N_{DD}^{+}. \tag{14}$$

The dark measurements and the carrier concentration observed after photoexcitation yield the shallow- and deep-donor concentrations. Therefore, only the thermal activation energy of the deep donor, E_{dd}, and the density of states, N_C, are unknown in Eqs. (13) and (14). In Fig. 3 the effective density of states in the L, Γ, and X valleys of $Al_xGa_{1-x}As$ are displayed for the entire alloy composition range. The density-of-states effective masses for electrons in the different valleys and the number of equivalent valleys in the plot of Fig. 3 were taken from Refs. 15 and 16. Furthermore, the joint density of states N_C^J (Ref. 9) is included in the plot. The joint density of states takes into account the distribution of electrons in all conduction-band minima.

Now we try to fit the calculated data obtained from the numerical solution of Eqs. (13) and (14) to the experimental data of the carrier concentration versus temperature in the dark for the samples depicted in Figs. 1 and 2. A good fit of experimental and calculated data is obtained

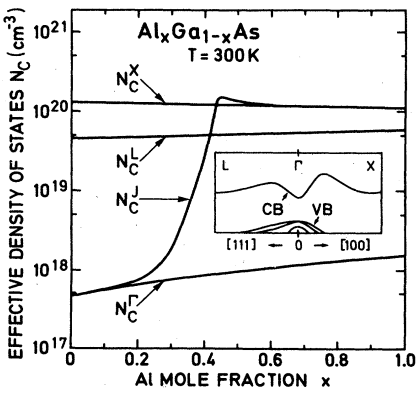

FIG. 3. Effective density of states at the bottom of the three conduction-band minima of $Al_xGa_{1-x}As$ versus alloy composition x. The joint density of states N_C^J which takes into account the distribution of electrons in several minima under thermal equilibrium conditions, is also included.

only if we take a value for the density of states which is much larger than the joint density of states. Inspection of Figs. 1 and 2 reveals that the agreement of experimental and calculated data is best, if an effective density of states of approximately $N_C \simeq 1.2 \times 10^{20}$ cm^{-3} is taken. The thermal activation energy of the deep donor is determined to be $E_{dd} = 130$ and 135 meV for the two compositions. This energy is in good agreement with the value obtained from the Eqs. (7) and (10). Consequently, if we assume the deep donor in n-type $Al_xGa_{1-x}As$:Si to be associated with a much larger density of states than that of the Γ valley we obtain good agreement of experiment and theory not only for the room-temperature carrier concentration, but also for the slope of the carrier concentration versus inverse temperature, and for the temperature at which the deep donor starts to be ionized.

In Fig. 1 we have also included the calculated curves if the joint density of states ($N_C = N_C^J$) is used in the calculation and the donor ionization energy is taken to be $E_{dd} = 130$ meV. However, it is impossible to obtain a reasonable fit with these parameters.

We can fit our experimental data by calculated data in the way described above only by means of a much larger density of states than the effective density of states of the Γ valley. Therefore we propose three possibilities of how such a large density of states enters the calculation. *First,* the conduction-band minima at the Γ and X points of the Brillouin zone have different linear temperature dependences. The donor energy is constant with respect to the X minimum, so that the deep-donor energy varies with temperature and respect to the energy of the conduction band at the Γ point. Assuming a linear temperature dependence of the conduction-band energy at the Γ point the deep-donor thermal ionization energy reads

$$E_{dd} = E_C^\Gamma + \alpha kT - E_{DD}. \tag{15}$$

The density of states [see also Eq. (6)] thus changes according to

$$N_C \exp[(E_C^\Gamma + \alpha kT - E_{DD})/kT]$$
$$= N_C \exp\alpha \exp[(E_C^\Gamma - E_{DD})/kT]. \tag{16}$$

In this way not the density of states N_C, but the modified density of states ($N_C \exp\alpha$), enters the calculation. *Second,* internal electric fields of the random alloy semiconductor play an important role, so that the density of states is influenced. Such internal electric fields are estimated on the basis of a theoretical model that we have recently developed to interpret luminescence linewidths.[17] According to this model the average magnitude of the internal electric field is estimated to be $E = 2.24 \times 10^3$ V/cm at an alloy composition of $x = 0.25$. The magnitude of this field is close to the Gunn-effect threshold field in GaAs.[18] The question of carrier heating and valley transfer by built-in electric fields is, however, problematic.[19,20] *Third,* the donor energy itself depends on temperature. In this case the density of states which enters the calculation can be much larger than the effec-

tive density of states of the Γ minimum according to Eqs. (15) and (16). A temperature-dependent donor energy is quite compatible with the concept of lattice distortion caused by the deep donor.[10]

The effect of persistent photoconductivity (PPC) is a characteristic property of n-type $Al_xGa_{1-x}As$ when $0.20 \leq x \leq 0.40$. The carrier concentration increases upon illumination and persists after the illumination. The measured photoexcited Hall electron concentration for the two representative samples of Fig. 1 and 2 remain constant for more than 48 h after switching off the illumination at 25 K without any noticeable decay of the carrier concentration. Since PPC is always observed in n-type $Al_xGa_{1-x}As$ with $x \simeq 0.3$, we believe that this effect originates from fundamental physical properties of the material rather than from a specific defect.

A localization of the deep-donor level in k space at $k \neq 0$ leads to a conclusive interpretation of PPC found in n-type $Al_xGa_{1-x}As$. Electron capture by the deep donor via the Γ valley is suppressed by a capture barrier[2,10] at low temperatures. We assume that the deep donor is most likely localized near the X point of the Brillouin zone, since the deep-donor concentration is correlated to the energy of the X valley (see Sec. III D). At low temperatures the deep donor is occupied, if the sample is cooled down in the dark. *Optical* excitation of the deep donor at low temperatures transfers an electron from the donor to the conduction band near the X point of the Brillouin zone. The electrons then transfer to the lowest-energy Γ valley and remain there at low temperatures.[21] The capture barrier which was estimated on the order of several hundred milli-electron-volts,[2] was explained by the configuration coordinate model,[10] which assumes a large lattice distortion proximate to the deep donor. The *thermal* activation of the deep donor, however, occurs most likely to the low-energy Γ valley, because the electron momentum need not be conserved during thermal ionization.

Non-Γ donors in semiconductors have already been discussed by Iseler *et al.*[22] for n-type CdTe and Paul[23] for GaSb. The interpretation of the PPC effect as a result of the peculiar *conduction-band* structure of $Al_xGa_{1-x}As$, i.e., the vicinity of the Γ and the satellite valleys also explains why PPC has never been observed in p-type $Al_xGa_{1-x}As$. Materials with a conduction-band structure similar to $Al_xGa_{1-x}As$, that is an upper indirect valley energetically close to the direct Γ valley, do in fact also exhibit PPC. In n-type GaSb,[24] e.g., the indirect L valley is close to the Γ valley. The occurrence of PPC in the binary compound semiconductor GaSb clearly demonstrates that PPC is not a property of a pseudobinary semiconductor *alloy*. Persistent photoconductivity is also observed in GaP_xAs_{1-x} near the Γ-L direct-indirect crossover point,[25] independent of the donor impurity. While $Al_xGa_{1-x}As$ is a cation alloy semiconductor, GaP_xAs_{1-x} is an anion alloy semiconductor.

The large variety of the chemical and the physical properties of the materials, which exhibit PPC and, on the other hand, the similarity of their conduction-band structure, strongly suggest that the peculiar localization of the deep donor in k space at $k \neq 0$, in addition to the lattice distortion, causes PPC.

D. Dependence of deep- and shallow-donor characteristics on alloy composition

In this section we discuss the transport properties of n-type $Al_xGa_{1-x}As$:Si as a function of alloy composition in the range $0 \leq x \leq 0.40$. First, the ratio of deep- and shallow-donor concentrations and their dependence on x are determined. Then the thermal activation energy of the deep donor is determined as a function of x with use of the procedure described in Sec. III C.

The deep donor freezes-out at low temperature, while the shallow donor does not freeze-out. For alloy compositions $x \leq 0.20$, no carrier freeze-out and no PPC effect is observed in n-type $Al_xGa_{1-x}As$ so that no deep Si donor is present in this alloy composition range. At a constant flux from the Si dopant effusion cell an increase of the Al-mole fraction leads to an increase of the concentration of the deep donor. For a qualitative estimate, note the difference between the PPC concentration and the low-temperature concentration in the dark, as depicted in Figs. 1 and 2.

In Fig. 4 we show the measured normalized ratio $(N_{SD}-N_{DD})/(N_{SD}+N_{DD})$ as a function of alloy composition x for highly doped samples ($N_{Si} \geq 1\times10^{17}$ cm^{-3}). The deep donor does not occur for $x \leq 0.20$ and dominates for $x \geq 0.35$. The shallow and the deep donor have the same concentration $N_{SD}=N_{DD}=\frac{1}{2}N_{Si}$ at an Al-mole fraction of approximately $x=0.27$. At a given alloy composition the *concentration* of the deep Si donor is proportional to the Si concentration, as also found for Te-doped n-type $Al_xGa_{1-x}As$.[10] The normalized *ratio* of the deep- and shallow-donor concentration, however, is independent of the Si concentration incorporated ($N_{Si} \geq 1\times10^{17}$ cm^{-3}).

The ratio of shallow- to deep-donor concentration does not change abruptly but rather continuously with alloy composition in the range $0.20 \leq x \leq 0.40$. We can correlate this behavior directly with the energy position of the Γ and the X valley. As the X valley comes down in ener-

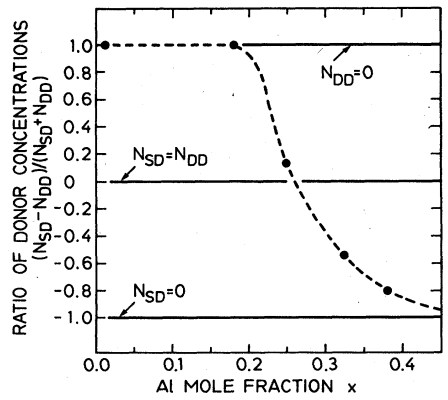

FIG. 4. Normalized ratio of shallow- and deep-donor concentration versus alloy composition x. At small Al-mole fractions, the Si concentration N_{Si} is equal to the shallow-donor concentration N_{SD}. The shallow-donor concentration is equal to the deep-donor concentration at an alloy composition of approximately $x=0.27$. At large Al-mole fractions the deep-donor concentration N_{DD} is approximately equal to the Si concentration N_{Si}.

gy and the Γ valley goes up smoothly with x, the deep-donor concentration increases, while simultaneously the shallow-donor concentration decreases, as depicted in Fig. 4. The deep donor is incompletely ionized at room temperature (see also Figs. 1 and 2). Therefore, since the concentration of the deep donor increases with the Al-mole fraction x, the Hall carrier concentration measured at 300 K decreases with x, even if N_{Si} is kept constant.[2,9,26]

Presence of the deep donor is observed in all our samples of alloy composition $0.20 \leq x \leq 0.40$. This donor occurs also if the n-type $Al_xGa_{1-x}As$ is doped with impurities other than Si [Se (Ref. 7), Sn (Ref. 9), and Te (Ref. 10)], although the chemical nature of the impurities is rather different. Si, for example, occupies a cation site, while Te occupies an anion site. Both impurities, however, act as donors. Furthermore, the deep donor occurs with different growth procedures [MBE, MOCV (Ref. 7), and LPE (Ref. 10)], even though the growth conditions and mechanisms are rather different. For MBE and MOCVD grown layers, the atomic As to Ga flux ratio is much larger than 1, while LPE layers are grown from a Ga-rich solution. Owing to the occurrence of the deep and shallow donor independent of the chemical property of the donor impurity and on the growth procedure, it is not probable that one specific defect is the origin of the microstructure of the deep level. We therefore assume that the nature of the shallow and deep donor is given by intrinsic properties of $Al_xGa_{1-x}As$.

Next we determine the dependence of the thermal activation energy of the shallow and the deep donor on the Al-mole fraction. This problem has been discussed controversially in previously published results.[7,9,26] The shallow donor, attached to the Γ valley, obeys the hydrogen-atom model in GaAs.[13] At high doping concentrations the shallow-donor activation energy is inaccessible in n-type GaAs and n-type $Al_xGa_{1-x}As$ by Hall measurements because the overlap of the wave function of the hydrogenlike impurities. In Fig. 5 we have therefore depicted the ground-state energy of the shallow donor, as calculated by the hydrogen-atom model, versus alloy composition. The shallow-donor ground-state energy gets slightly deeper with increasing Al-mole fraction due to the small change of the effective mass in the Γ valley.[16] This calculated deepening of the shallow donor was recently confirmed by our photoluminescence measurements.[27]

The thermal activation energy of the deep donor is evaluated in terms of Fermi-Dirac statistics (see Sec. III C) by fitting the calculated and experimental data. We investigated a large number of n-type $Al_xGa_{1-x}As$:Si samples with different Al content and the results are depicted in Fig. 5. The important result is that the deep-donor activation energy does *not* change significantly with Al-mole fraction x. For the direct composition range of $Al_xGa_{1-x}As$ ($0.20 \leq x \leq 0.40$) we obtain a value of 140 ± 10 meV. This result is in contrast to previous studies.

We can also use the relation $n^2 - nN_{SD} \sim \exp(-E_{dd}/kT)$ [Eq. (7)] to determine the thermal activation energy of the deep donor. For large Al-mole fractions, where the deep donor dominates ($x \geq 0.35$), the Hall electron concentration at room temperature is much

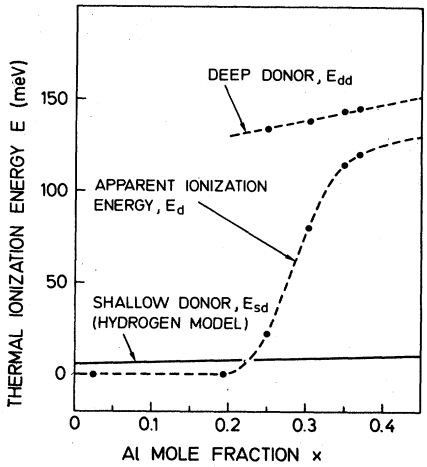

FIG. 5. Dependence of the thermal activation energy of the deep donor E_{dd} versus alloy composition x. The shallow-donor ground-state energy according to the hydrogen-atom model is also included. The apparent thermal activation energy E_d, which is obtained using the relation $n \sim \exp(-E_d/2kT)$ is included as well.

larger than the shallow-donor concentration, i.e., $n \gg N_{SD}$. Therefore, Eq. (7) can be approximated by $n \sim \exp(-E_{dd}/2kT)$ which corresponds to Eq. (2b). For Al-mole fractions where the shallow donor is dominant, this simple relation largely underestimates the thermal activation energy because the contribution of the shallow donor is neglected. The thermal ionization energy derived by this formula will therefore be called *apparent* activation energy E_d as illustrated in Fig. 5, versus alloy composition. Inspection of Fig. 5 reveals that the apparent activation energy E_d clearly increases strongly with increasing Al-mole fraction, as found previously by several authors.[7,9,26] The statement that the thermal activation energy of the donor in n-type $Al_xGa_{1-x}As$ increases with increasing Al-mole fraction, i.e., the donor is deepening, is therefore false. The interpretation is due to the change of the ratio of shallow- to deep-donor concentration. We believe that there are in fact two donors in n-type $Al_xGa_{1-x}As$ for alloy compositions $x \geq 0.20$. The thermal activation energy of the deep donor is determined to be 130—135 meV, at an alloy composition of $0.20 \leq x \leq 0.30$. The activation energy is determined to be 140—150 meV at an alloy composition of $0.35 \leq x \leq 0.40$. The deep-donor thermal activation energy thus slightly deepens with alloy composition. In a first-order approximation, however, the deep-donor thermal activation energy does not depend significantly on x and is determined to be 140 ± 10 meV in the composition range $0.20 \leq x \leq 0.40$. The concentration of the deep donor N_{DD} increases with x while, simultaneously, the shallow-donor concentration N_{SD} decreases, and this implies an apparent variation of E_d with x if deduced via Eq. (2a) or (2b).

In Fig. 6 we show the energy position of the conduction-band edges of the L, Γ, and X minima as function of the alloy composition.[16] Furthermore, we have included the donor levels below the respective bands.

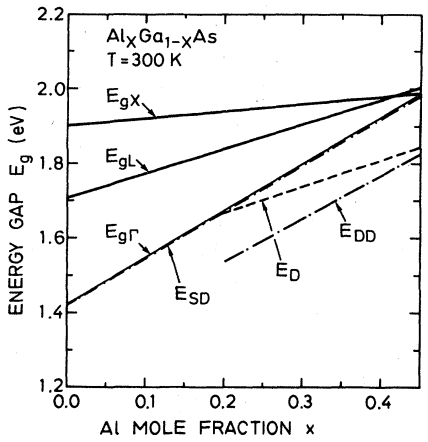

FIG. 6. Energies of the Γ, L, and X valleys in $Al_xGa_{1-x}As$ versus Al-mole fraction x. The energy of the hydrogen-atom-like shallow donor as well as the activation energy of the deep donor below the Γ minimum energy are included in the plot. The apparent ionization energy E_d, which follows from the relation $n \sim \exp(-E_d/2kT)$ is also plotted.

The shallow donor follows the Γ minimum according to the hydrogen-atom model and the effective-mass approximation. The thermal activation energy of the deep donor below the Γ minimum is roughly constant with respect to x. The thermal activation energies plotted in Fig. 5 do *not* represent the ground-state energy,[11] as already mentioned. The apparent thermal activation energy E_d is also included in the plot. Obviously this energy follows the L minimum as discussed in Ref. 28. This finding, however, is due to the procedure used for evaluation of the activation energy.

IV. CONCLUSION

We have in detail evaluated experimental data obtained from temperature-dependent Hall-effect measurements on n-type $Al_xGa_{1-x}As$:Si of composition $0 \leq x \leq 0.40$ grown by molecular-beam epitaxy (MBE) and heavily doped with silicon $N_{Si} \geq 5 \times 10^{17}$ cm^{-3}. Our quantitative analysis, using Fermi-Dirac statistics, revealed that in the composition range $0.20 \leq x \leq 0.40$ both a hydrogenlike shallow Si donor which interacts with the Γ valley and a deep Si donor are present in the ternary material. The ratio of shallow- to deep-donor concentrations depends strongly on alloy composition. For $x \leq 0.20$ no deep donor and no persistent photoconductivity (PPC) exist in n-type $Al_xGa_{1-x}As$. For $0.20 \leq x \leq 0.40$, however, the deep-donor concentration increases with x while simultaneously the shallow-donor concentration decreases. Furthermore, the thermal activation energy of the deep donor cannot be derived from the frequently used simple exponential relation $n \sim \exp(-E_{dd}/kT)$, because the concentration of the shallow donor is not included. The E_{dd} values represent only apparent donor activation energies arising from an averaging of the actual deep- and shallow-donor levels and their respective concentrations at a given alloy composition. Three methods have been used to determine the donor activation energy from the temperature-dependent Hall-effect data for the alloy composition range $0.20 \leq x \leq 0.40$: (i) statistic considerations, (ii) law of mass action, and (iii) application of Fermi-Dirac statistics for the donor as well as for the conduction band. All three methods yield a value of $E_{dd} = 140 \pm 10$ meV for the thermal activation energy of the deep donor in n-type $Al_xGa_{1-x}As$:Si. The value of $E_{dd} = 140 \pm 10$ meV remains roughly constant in the whole composition range $0.20 \leq x \leq 0.40$. This is in contrast to previously published results where a pronounced deepening of the donor level with x as derived from the misleading relation $n \sim \exp(-E_{dd}/kT)$ has been reported. Finally we show that the proposed interaction of the deep donor with the X valley together with the configuration coordinate model explains the effect of persistent photoconductivity (PPC) in n-type $Al_xGa_{1-x}As$ whose intensity is proportional to the doping concentration and to the layer thickness.

ACKNOWLEDGMENTS

The authors would like to thank A. Fischer and J. Knecht for expert help in sample preparation. We are indebted to H. J. Queisser, Y. Horikoshi, H. Kroemer, and P. H. Roth (Universität Stuttgart, Institut G. Kohn) for much useful advice and critically reading the manuscript.

[1] T. J. Drummond, W. G. Lyons, R. Fischer, R. E. Thorne, H. Morkoc, C. G. Hopkins, and C. A. Evans, Jr., J. Vac. Sci. Technol. **21**, 957 (1982).

[2] H. Künzel, A. Fischer, J. Knecht, and K. Ploog, Appl. Phys. A **32**, 69 (1983).

[3] T. Ishibashi, T. Tarucha, and H. Okamoto, Jpn. J. Appl. Phys. **21**, L476 (1982).

[4] K. Hikosaka, T. Mimura, and S. Hiyamizu, *Gallium Arsenide and Related Compounds, Oiso, 1981,* edited by T. Sugano (IOP, Bristol, 1982), p. 233.

[5] H. Künzel, K. Ploog, K. Wünstel, and B. L. Zhou, J. Electron. Mater. **13**, 281 (1984).

[6] D. M. Collins, D. E. Mars, B. Fischer, and C. Kocot, J. Appl. Phys. **54**, 857 (1983).

[7] J. J. Yang, L. A. Moudy, and W. I. Simpson, Appl. Phys. Lett. **40**, 244 (1982).

[8] R. J. Nelson, Appl. Phys. Lett. **31**, 351 (1977).

[9] K. Kaneko, M. Ayabe, and N. Watanabe, *Gallium Arsenide and Related Compounds, Edinburgh, 1976,* edited by C. Hilsum (IOP, Bristol, 1977), p. 216.

[10] D. V. Lang, R. A. Logan, and M. Jaros, Phys. Rev. B **19**, 1015 (1979).

[11] R. Dingle, R. A. Logan, and J. R. Arthur, *Gallium Arsenide and Related Compounds, Edinburgh, 1976,* edited by C. Hilsum (IOP, Bristol, 1977), p. 210.

[12] G. Abstreiter, E. Bauser, A. Fischer, and K. Ploog, Appl. Phys. **16**, 345 (1978).

[13] G. E. Stillman and C. M. Wolfe, Thin Solid Films **31**, 69 (1976).

[14] W. B. Joyce and R. W. Dixon, Appl. Phys. Lett. **31**, 354 (1977).

[15] J. S. Blakemore, J. Appl. Phys. **53**, R123 (1982).

[16]H. C. Casey and M. B. Panish, *Heterostructure Lasers* (Academic, New York, 1978).
[17]E. F. Schubert, E. O. Göbel, Y. Horikoshi, K. Ploog, and H. J. Queisser, Phys. Rev. B **30**, 813 (1984).
[18]J. G. Ruch and G. S. Kino, Appl. Phys. Lett. **10**, 40 (1967).
[19]J. B. Gunn, J. Appl. Phys. **39**, 4602 (1968).
[20]R. Stratton, J. Appl. Phys. **40**, 4582 (1969).
[21]K. Seeger, *Semiconductor Physics* (Springer, Berlin, 1982), p. 232.
[22]G. W. Iseler, J. A. Kafalas, A. J. Strauss, H. F. MacMillan, and R. H. Bube, Solid State Commun. **10**, 619 (1972).
[23]W. Paul, in *IX International Conference on the Physics of Semiconductors, Moscow, 1968,* edited by S. M. Ryvkin (Nauka, Leningrad, USSR, 1968), p. 16.
[24]L. Dmowski, M. Baj, M. Kubalski, R. Piotrzowski, and S. Porowski, *Proceedings of the 14th International Conference on the Physics of Semiconductors, Edinburgh, 1978,* edited by B. L. H. Wilson (IOP, Bristol, 1978), p. 417.
[25]M. G. Craford, G. E. Stillman, A. Rossi, and N. Holonyak, Jr., Phys. Rev. **168**, 867 (1968).
[26]A. J. SpringTorpe, F. D. King, and A. Becke, J. Electron. Mater. **4**, 101 (1975).
[27]H. Jung, A. Fischer, and K. Ploog, Appl. Phys. A **33**, 9 (1984).
[28]P. K. Bhattacharya, A. Majerfeld, and A. K. Saxena, *Gallium Arsenide and Related Compounds, St. Louis, 1978,* edited by C. M. Wolfe (IOP, Bristol, 1979), p. 199.